

Training Noise Token Pruning

Mingxing Rao, Bohan Jiang, Daniel Moyer
Vanderbilt University
Nashville, TN 37235, USA

{mingxing.rao, bohan.jiang, daniel.moyer}@vanderbilt.edu

Abstract

In the present work we present Training Noise Token (TNT) Pruning for vision transformers. Our method relaxes the discrete token dropping condition to continuous additive noise, providing smooth optimization in training, while retaining discrete dropping computational gains in deployment settings. We provide theoretical connections to Rate-Distortion literature, and empirical evaluations on the ImageNet dataset using ViT and DeiT architectures demonstrating TNT's advantages over previous pruning methods.

1. Introduction

Token pruning is a class of methods for reducing computational load in transformers [20] by reducing the input length. While transformers are already somewhat robust to dropping a small number of tokens at random, learned dropping schemes enable larger dropping rates and thereby higher speed-ups with smaller accuracy penalties. These gains are only amplified by operations super-linear cost scaling (e.g., attention) and memory footprint.

Token pruning methods exploit predictive information differences between tokens; for a given task, some tokens are more useful than others. By dropping the least informative tokens first, a learned method can preserve the most amount of accuracy while removing desired number of tokens. While these methods were originally explored in a natural language processing context, token redundancy is arguably stronger in image transformers, and multiple token pruning methods for vision models (e.g. ViT [8]) have been proposed [15, 17, 21–23]. Unfortunately, token pruning as an action is discrete and not easily optimized directly. Current techniques use either forms of stochastic discrete dropping [17, 23], or heuristics [21] using attention activations themselves.

In this paper, we reframe Token Pruning as a constrained case of the Information Bottleneck problem. By viewing the token dropping rate as a channel constraint and the accuracy penalty as a distortion metric, we can directly apply ideas

from the compression literature. Relaxations of these conditions provide continuous optimization desiderata, which are more easily optimized. Even though the original problem is difficult to solve exactly due to high-order token interaction information (“synergy” and “redundancy”), we show that a simple approximation to this case works surprisingly well. Specifically, we demonstrate that the proposed method has superior performance in comparison to recent pruning methods using either stochastic discrete dropping or attention heuristics on standard base models for the ImageNet-1K benchmark, in particular in the low token regime (i.e., when removing a large percentage of tokens).

In the present work we provide:

- A novel method for token-pruning that provides state-of-the-art performance with respect to the accuracy/computation load trade-off.
- A justification and intuition for that method based on the information bottleneck.
- Empirical experiments demonstrating the use and utility of our method along with previous methods as baselines, with evaluations on ImageNet [8] using two common image transformers, ViT [8] and DeiT [19], as base architectures. Our code can be found at <https://github.com/mx-ethan-rao/tnt>.

2. Related Work

Token Pruning: Token pruning (or “token dropout”) has been explored for both transformer-based language models [10, 12, 13] and vision transformers [17, 21–23]. Broadly speaking, these methods can be separated into two categories: stochastic dropout methods, where tokens are randomly removed based on a per-token computed likelihood [10, 12, 13, 17, 23], and heuristic attention-based methods [15, 21]

Rao et al. 2021 [17] introduces Dynamic ViT, which is notable as the first token pruning method for vision transformer [8]. It is prototypical of the stochastic dropout family of methods: it defines a relaxation of the rate criterion and samples tokens according to an inclusion likelihood. Yin et al. 2022 [23] introduce a refinement of this method (Adaptive

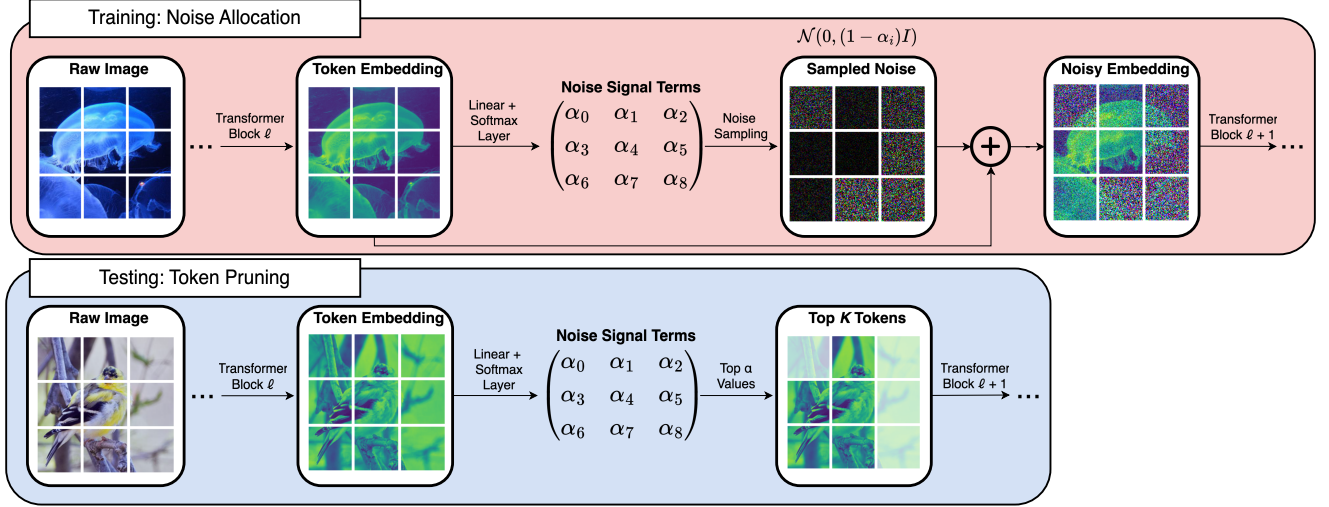


Figure 1. **Training Noise Token Pruning (TNT)**. Our proposed method computes a relevance term α_i for each token. In training (diagrammed at top), these terms dictate an amount of noise added to the token, while at test time they indicate pruning order.

ViT), incorporating a halting module and associated score, as well as a loss function that encourages early stopping.

Along a different path, multiple heuristics have been introduced for token pruning based on the attention scores [15, 21]. These use the intuition that tokens to which other tokens ascribe high attention (highly attended tokens) are of high importance. Liang et al. 2022 [15] additionally merges the lowest attended tokens, while Wang et al. 2024 puts this both into a graph ranking framework (PageRank [16]) and into the zero-shot context.

A simple baseline version of an attention-based heuristic, “Top-K pruning”, was also found to perform competitively as well [11]. This method simply ranks tokens based on the attention distribution to a CLS token, and then truncates after the top K . While it is not directly applicable to architectures without CLS tokens or non-classification tasks, our results in Section 4 show that it outperforms most other methods where it can be applied.

Merger Methods: Complementary to dropping methods, token mergers and similarity-based pruning methods also decrease transformer computational cost by reducing the size of the token set [5, 15, 21]. Similarity-based pruning [21] exploits exactly the opposite problem in the token set; instead of removing low relevance tokens they generally merge redundant tokens. Merger methods are more general, also possibly allowing for encoding of background context variables [5]. The use of these methods is not mutually exclusive with token pruning [21]. While in the present work we do not provide a completely novel merger method, we provide improvements on an existing similarity-based pruning step, and provide justification for its necessity.

Information Bottleneck: Our framework for token dropping relies upon theory originally explored in the Information Bottleneck [2, 18], which in turn is based upon Rate-Distortion theory [3]. The information bottleneck characterizes encodings in terms of their relevance (the additive inverse of a distortion metric) and a rate constraint. We place token pruning’s two relevant metrics into this context, which then provides a natural relaxation for the rate constraint.

3. Methodology

3.1. Token pruning as bottleneck optimization

We model token pruning optimization as a set selection problem. Given a transformer architecture f , we want to select the token subset $T \subset \mathcal{T}$ that minimizes loss \mathcal{L} for each data-point and label pair (x, y) subject to constraint $|T| < K$:

$$\min_{T \subset \mathcal{T}} \mathcal{L}(f(x|_T), y) \text{ s.t. } |T| < K \quad (1)$$

where \mathcal{T} is the set of all tokens, and $x|_T$ are input data restricted to the token set T .

We can map this problem into the information-theoretic literature by drawing analogies between the loss and constraint functions in Eq. 1 and the rate and distortion functions of compression literature [18]. The loss function usually measures discrepancies between y and its estimator $f(x|_T)$, and, as in previous work [2, 18], is a direct analog to the distortion function.

The analog to the rate function requires more assumptions. While viewing each token as a fixed number of bits directly maps the $|T| < K$ constraint into a transmission rate, this does nothing to aid our optimization. Taking the mapping one step further, we could instead use the mutual

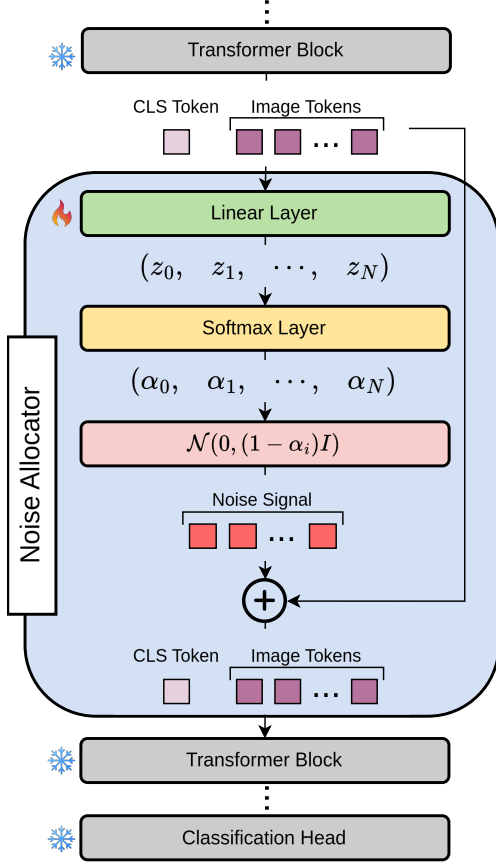


Figure 2. **Noise Allocator block architecture:** the block diagrammed above is injected into pre-trained models as a pruning layer. It takes the output of the previous Transformer block as input, then computes the noise signal terms α using a linear layer followed by a Softmax function. During training it samples Gaussian noise conditioned on α for each token, then adds the noise to the token embeddings. At test time, tokens are instead dropped. This pruning method can be trained with all parameters outside the noise allocator are frozen.

information $I(x|_T, x) < K$ constraint. This forces the effective information transmission to remain below K bits. We then would like to solve

$$\min_{T \subset \mathcal{T}} \text{Distortion}(f(x|_T), y) \text{ s.t. } I(x|_T, x) < K \quad (2)$$

which is exactly the Information Bottleneck.

This formulation is at once quite useful in that it maps a discrete optimization into a continuous problem, yet unfortunately also problematic in its exact computation. The rate parameter is definitionally aware of the content of the tokens. This provides us with a route to a potential procedure: force the token content to have at most K bits of information from the original x by adding an external source of noise. Selecting what information to keep from x is equivalent to

token selection, but still enjoys a continuous optimization landscape, so long as we choose to add continuous noise. On the otherhand, in order to exactly measure the mutual information we need to measure redundancy between tokens. This issue also was implicitly present in the discrete form of the optimization problem, but it is explicitly included in mutual information.

3.2. Proposed approximate solution

Solutions to the information bottleneck have been proposed in the literature, both in a general setting [18] and in a deep learning context [1, 2]. However, for token pruning, these solutions are almost certainly too computationally heavy to be efficient as dropping methods. Instead, we will solve a simplified version that ignores redundant information, then prune redundant tokens in a second phase. Surprisingly, even with the errors induced by approximation, this method produces accurate results with very little compute overhead.

Given a non-pruned vision transformer architecture, we train a module we call the Noise Allocator to estimate relative token relevance scalars α_i for each token. Due to the residual connections used by many transformer architectures, this module can be placed after any of the individual transformer blocks, or after multiple blocks (in a multi-layer dropping case).

Consider an architecture with L repeated transformer blocks possibly after an initial token embedding layer (for example, ViT has 12 identical blocks). Let the ℓ th Transformer block $f^{(\ell)}$ with input $x \in \mathbb{R}^{N \times D}$, where N is the number of tokens, and D is the embedding dimension. Let $x_i^{(\ell)}$ denote the i th token. For every block where the user would like to perform pruning, we introduce a linear token relevance predictor with a weight matrix $W^{(\ell)} \in \mathbb{R}^{D \times 1}$.

We then compute α_i as

$$\alpha_i^\ell = \text{Softmax}(W^{(\ell)} f^{(\ell)}(x^{(\ell)})) \quad (3)$$

For training/fine-tuning, we compute noise variables η_i^ℓ as

$$\eta_i^\ell = (1 - \alpha_i^{(\ell)})\varepsilon, \quad (4)$$

where $\varepsilon \sim \mathcal{N}(0, \beta I_D)$ (“the reparameterization trick” [14]). Here, β is a hyper-parameter that controls the total amplitude of noise added, and corresponds with K up to a monotonic transformation. The Softmax function in Eq. 3 ensures that the network must allocate β amount of noise; without it, a degenerate zero-noise solution exists.

Classical results in Information Theory state that the mutual information (channel capacity) for each token to its noised variant has an upper bound proportional to $\log(1 + P_{\text{signal}}/P_{\text{noise}})$, where $P_{\text{signal}}/P_{\text{noise}}$ is the ratio of the power (amplitude) of the token signal and to that of the noise [6] (the signal to noise ratio). Due to the layer-wise

normalization (LayerNorm) of many transformer architectures, P_{signal} is necessarily bounded. Disregarding the synergistic information between tokens, optimizing our proposed Noise Allocator amounts to solving an information bottleneck problem. We discuss limitations of this approach in Section 4.4.

At test time noise is not sampled, and instead of β we directly select the top K tokens, dropping the rest of the token set. We interpret $\alpha^{(\ell)}$ as a token importance map for $x^{(\ell)}$. Based on this importance ranking, we may either discard less important tokens or merge them with other tokens in the subsequent stage.

Weight vector W is applied to every x_i identically, so the additional parameter space complexity remains $\mathcal{O}(NL)$, where L is the number of layers at which tokens are selectively dropped during testing. Given $L \ll D$, this complexity effectively reduces to $\mathcal{O}(D)$, making it comparatively negligible within the overall model size. For weaker encoders and/or smaller transformer blocks such as DeiT-Tiny, it is sometimes helpful to increase the complexity of W to a multi-layer structure (e.g., an MLP), as we show in experiments in the Appendix.

3.2.1. Similarity-based Pruning by Random Partition (Redundancy Removal)

Even though individual tokens might be highly relevant to the classification problem (i.e, individually $I(x_i^\ell, y)$ might be high), relevant tokens sharing a high amount of information with a kept token represents wasted capacity. In order to avoid this waste, we implement a redundancy removal step for test time usage, which removes similar and therefore possibly redundant tokens.

The method is as follows: Tokens are randomly divided into two groups. We then identify the closest matching token in one group for each token in the other, recording the similarity scores of each paired token based on their token embeddings. Next, we prune the top- r most similar pairs and prune the associated tokens in the second group.

Our similarity-based pruning approach closely resembles that of Zero-TP [21], with two key modifications. First, rather than using the Key values as the partitioning metric, we directly use $x^{(l)}$ so that it can be applied directly after the Noise Allocator step. Second, instead of sequentially partitioning tokens based on their importance scores, we apply a random partitioning strategy. Our ablation study suggests that random partitioning yields improved performance for the proposed model.

4. Experiments

We conduct a series of experiments on pre-trained vision transformer models, including DeiT (Tiny¹, Small,

Base) [19] and ViT/16 [8], each trained on ImageNet-1K [7]. We then compare our model with previously proposed token-dropping models, as well as two simple baseline schemes: DynamicViT [17], ZeroTP[21], ToMe [5], Top-K [11], and random dropping. In Section 4.3, we present ablation studies to validate our individual design choices.

We first show qualitative results for pruning 50% of tokens at varying layers (single-layer pruning at layers 1-5) on the ImageNet-1K validation dataset in Figure 3. As seen at left in the figure, extremely early layers result in relevant tokens being dropped, and irrelevant tokens being included; this matches with results from previous literature [9, 17, 21]. Results further indicate that the importance score based on noise signal term α becomes more reasonable in latter layers, performing well on a variety of qualitatively different images (tiny objects, mixed foreground and background, low contrast separation). Additional examples are provided in the Appendix.

We conduct a comprehensive evaluation for each method by sweeping the token keep rate (K) from low to high-token regime, as detailed in Sections 4.1 and 4.2. We experiment with both single-layer and multi-layer pruning schema. In the single-layer scheme all token pruning occurs at a single layer, usually early in the network. In comparison, the multi-layer scheme has pruning blocks spread across the architecture. The multi-layer scheme is generally more effective, albeit with additional computational cost, but due to the large number of possible parameters for multi-layer pruning introduced by the multiple keep rates (with possibly varying predictive accuracy), may be hard to effectively tune for all methods. This makes comparisons in the multi-layer scheme inexact, which is why we include the single layer experiments. We evaluate each model in terms of Top-1 Accuracy, FLOPs, and throughput. Our model achieves top performance across most experiments and remains competitive on others.

Experimental Setup: All training and evaluations are conducted on a single compute node equipped with 8 NVIDIA A40 GPUs. The experiments are performed on the ImageNet-1K dataset [7], with all images resized to a resolution of 224px. We evaluate the proposed method using only frozen pre-trained backbone methods, training the Noise Allocator weights for 40 epochs. And we set β (a hyperparameter controlling the magnitude of added noise) to 0.02 for all base models while training. For testing, a single GPU to measure the computational performance.

4.1. Rate Sweep for Single Layer Pruning

The experiments of previous studies have shown that most models [9, 17, 21] refrain from dropping tokens in initial Transformer layers, as these layers contain limited information relevant to token importance. For our experiments, we select the second layer for ViT and third layer for DeiT

¹DeiT-Tiny results relegated to the Appendix.

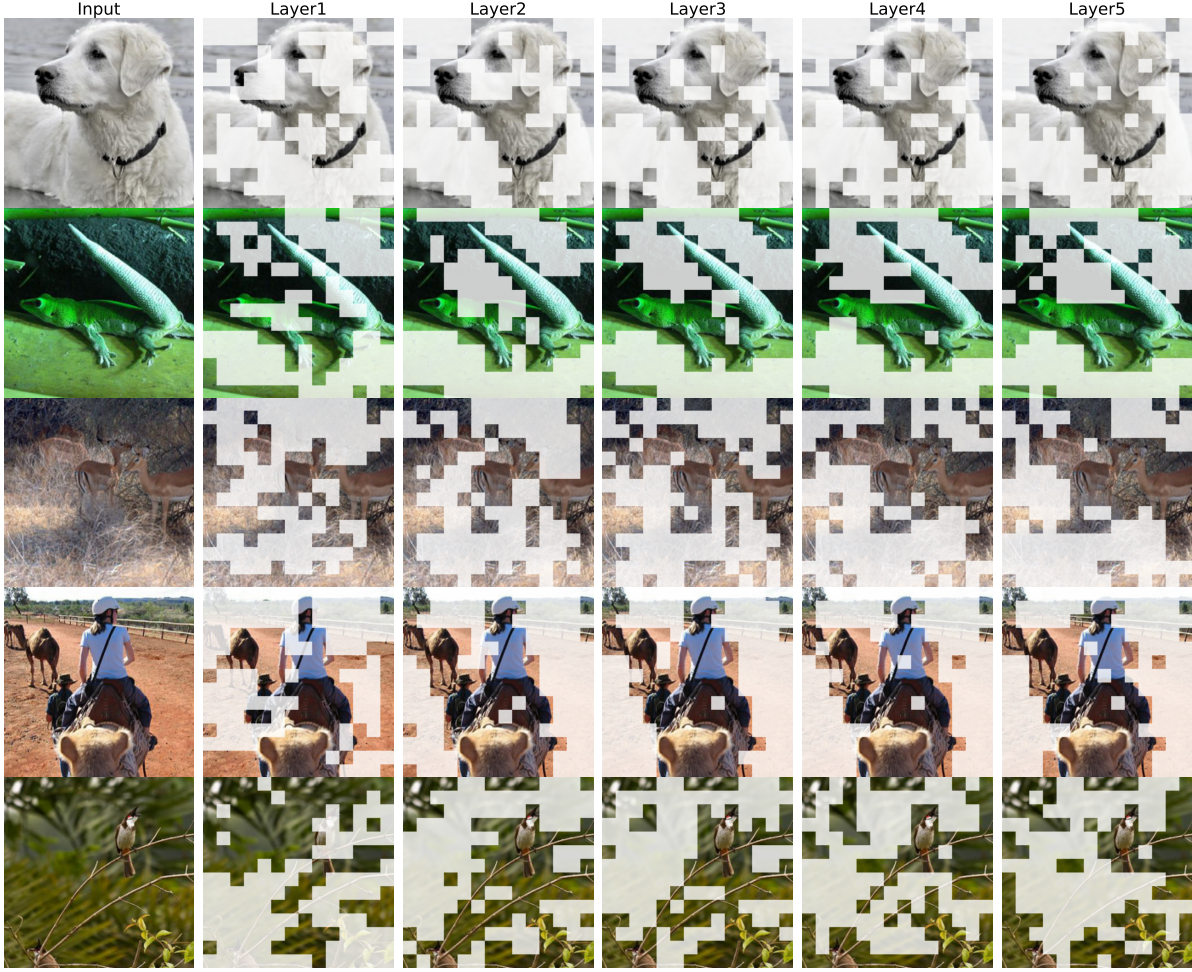


Figure 3. Visualization of Token Pruning maps on ImageNet-1K: at **left** are the original images, and at each column **progressing right** are single layer prunings and their associated kept/dropped tokens, for layers 1-5 of the DeiT-B-Distil. model.

variants as the standard layers for single-layer token pruning. We use the standard pre-trained DeiT variants for all experiments for all models. For all ViT experiments for all models, we use a modified ViT/16 with smaller embedding dimension $mlp_dim = emb_dim = 768$. Additionally, we use mean-pooled token embeddings for predictions instead of the CLS token.

Plots for pruning performance on DeiT-S-Dist., DeiT-B-Dist., ViT/16 across different pruning models are presented in Figure 4, for both Top-1 Accuracy versus GFLOPs and Top-1 Accuracy versus throughput (images per second). In general throughput is not one-to-one with GFLOPs due to differing parallelism between models. Performance between all methods converge to the base model case as the keep rate approaches 1.0. For decreasing K however, the proposed model shows superior performance until $K \leq 0.25$, at which point baseline models overtake the proposed model, albeit with all models experiencing strong performance degradation. In general our results for the baseline models mirror

that of Haurum et al. 2023 [11], and similar to their report we also find that the Top-K baseline is generally the strongest where it can be applied (i.e., for models incorporating the CLS token), aside from our proposed method.

Overall, the number of tokens pruned is consistent across models for a given keep rate. For TNT, we select top $(NK + s)$ at the Noise Allocator stage and prune s tokens at the similarity pruning stage for a given keep rate K and total number of tokens N . We set s to be 25 and 30 for experiments involving DeiT and ViT, respectively. We apply the same setting to Zero-TP [21], as it also utilizes similarity-based pruning. We could not reproduce the results of Yin et al. [23] in our own experimental context. In Table 1, we report specific numerical results for ViT/16 and DeiT-S-Distl, contingent on keep rates K , instead of GFLOPs or Throughput as in the plots. Complete numerical results and details such as keep rates for each experiment are also provided in the Appendix. For ToMe [5], it is impossible to prune more than 50% of tokens within a single layer, so lower

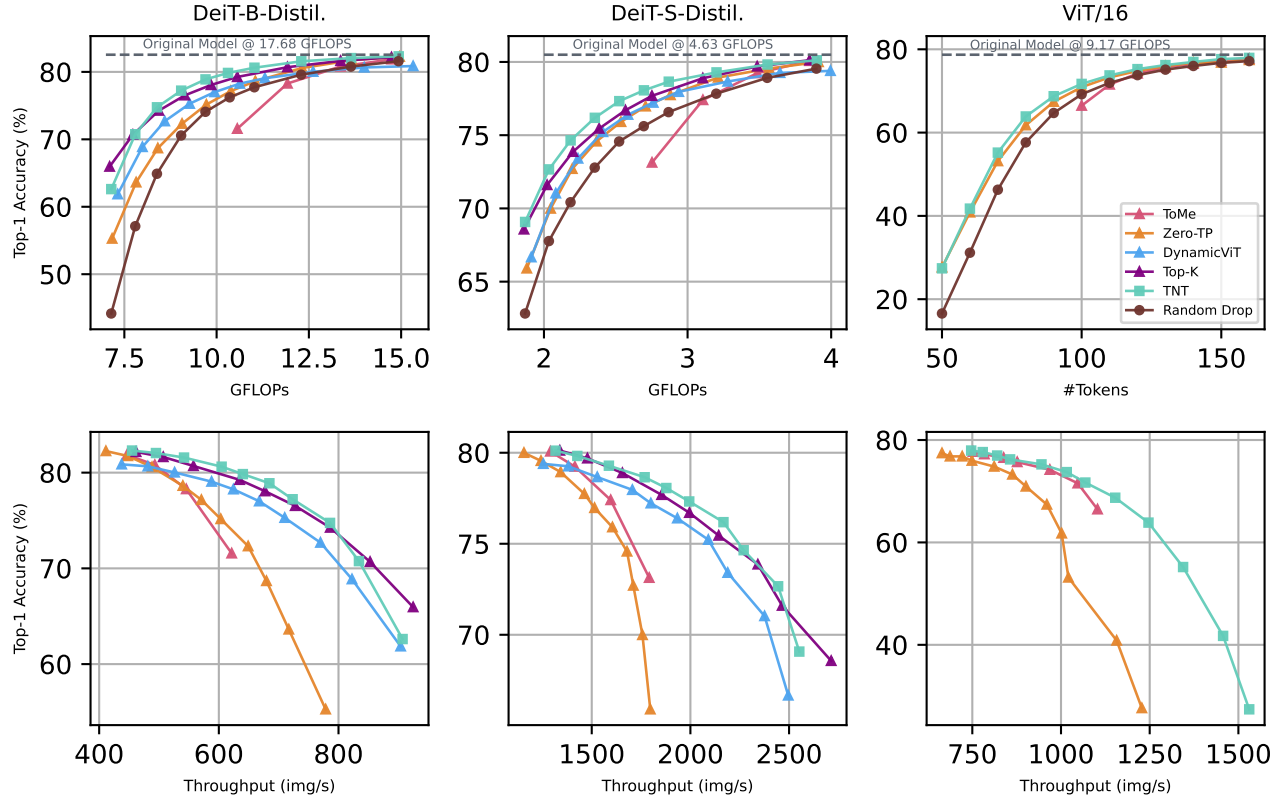


Figure 4. **Single Layer Pruning results:** We plot the Top-1 Accuracy in the ImageNet-1k validation set for each of the pruning methods as a function of computational efficiency, in the **top row** measured by GFLOPs and in the **bottom row** measured by throughput, for **single layer pruning**. The base model is DeiT-B-Distil in the **first column**, DeiT-S-Distil. in the **second column**, and ViT/16 in the **third column**.

	K=1.0		K=0.8		K=0.6		K=0.5		K=0.25	
	#tokens=196		#tokens=156		#tokens=127		#tokens=98		#tokens=49	
	Acc.	GFLOPs	Acc.	GFLOPs	Acc.	GFLOPs	Acc.	GFLOPs	Acc.	GFLOPs
DeiT-S-Distil.										
Random Drop	80.50	4.63	79.54	3.90	77.83	3.20	76.57	2.87	67.77	2.03
ToMe [5]	–	–	80.07	3.85	77.40	3.11	73.13	2.75	–	–
Zero-TP [21]	–	–	80.00	3.91	78.94	3.21	77.74	2.88	69.99	2.05
DynamicViT [17]	–	–	79.39	3.99	78.66	3.28	77.96	2.94	71.03	2.08
Top-K [22]	–	–	80.12	3.85	78.89	3.11	77.69	2.75	68.57	1.86
TNT (ours)	–	–	80.11	3.90	79.29	3.20	78.65	2.87	72.66	2.03
ViT/16										
	#tokens=196		#tokens=160		#tokens=130		#tokens=100		#tokens=60	
	Acc.	GFLOPs	Acc.	GFLOPs	Acc.	GFLOPs	Acc.	GFLOPs	Acc.	GFLOPs
Random Drop	78.70	9.17	77.17	7.69	75.12	6.50	69.21	5.33	31.16	3.81
ToMe [5]	–	–	77.71	7.66	75.70	6.42	66.46	5.22	–	–
Zero-TP [21]	–	–	77.43	7.32	75.96	6.52	70.92	5.35	40.84	3.83
TNT (ours)	–	–	77.94	7.70	76.22	6.50	71.69	5.33	41.75	3.81

Table 1. Top-1 Accuracy on the ImageNet-1K validation set (Acc.) and computational cost (GFLOPs) across methods for differing keep rates K , using a single layer of token pruning. The **left most column** are the performance and computational cost of the base architectures.

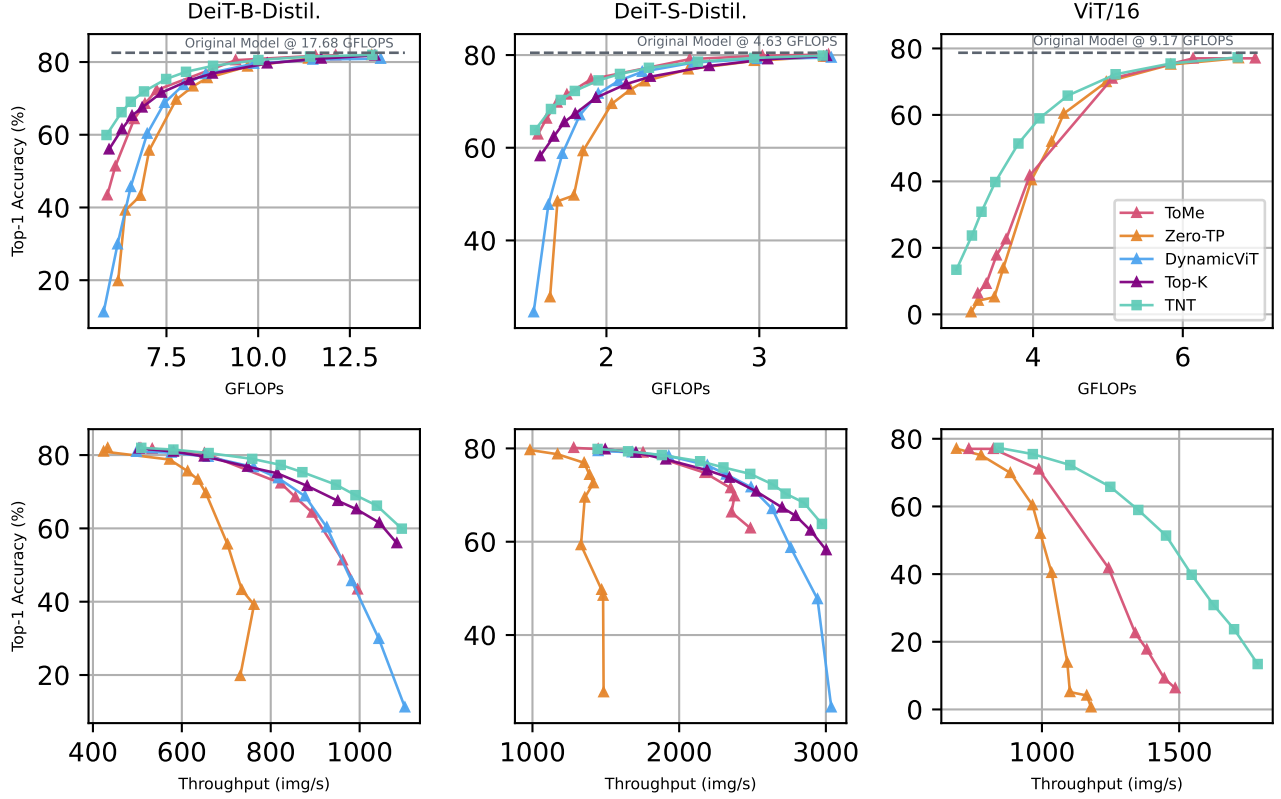


Figure 5. **Multi-layer Pruning results:** We plot the Top-1 Accuracy in the ImageNet-1k validation set for each of the pruning methods as a function of computational efficiency, in the **top row** measured by GFLOPs and in the **bottom row** measured by throughput, for **multi-layer pruning**. The base model is DeiT-B-Distil in the **first column**, DeiT-S-Distil. in the **second column**, and ViT/16 in the **third column**.

single-layer pruning is not possible.

4.2. Rate Sweep at Multi-layer Pruning

We evaluate the performance of token pruning across multiple layers as this better reflects a performant pruning system, with the caveat that equal comparison conditions are more difficult to ensure. For the token keep rate at each layer and the specific layers chosen for token pruning (i.e. pruning locations), we strictly follow the instructions on the original paper for each model. For Zero-TP [21], tokens are pruned at layers [1, 3, 6, 9, 11], where layers [1, 11] perform similarity-based pruning only; for ToMe [5], pruning occurs at every layer; and for DynamicViT [17], pruning is applied at layers [3, 6, 9]. As Top-K lacks specific pruning instructions, we align its pruning layers with those of TNT. We gradually sweep the keep rate at pruning locations to generate Figure 5 for DeiT-B-Distil., DeiT-S-Distil., and ViT/16. We also provide partial numerical results in Table 2. All base models are the same as those used in the single-layer pruning section. Additional details on experimental setups and specific details for each model are provided in the Appendix.

For TNT, we prefer pruning tokens at earlier layers, as it provides stronger performance, and as shown in Figure 3, layers [3, 4, 5] serve as effective locations for token pruning. Rather than performing the similarity pruning stage at every pruning layer as in Zero-TP, we prune s tokens before tokens are sent to the ViT blocks. Our ablation study justify this. For all experiments, s is set to 40. Our results indicate that TNT consistently shows strong performance in varying token (computation) ranges. As the proportion of pruned tokens increases, the importance of the retained tokens becomes more critical. TNT shows a larger performance gap compared to other models in the low-token regime.

4.3. Ablation Study

We conducted an ablation experiment to justify inclusion of the similarity-based pruning by random partition, as opposed to token merger or sequential partition. We find a slight boost to performance with similarity based pruning, with a very minor bias towards the random partition method. Previous works [4, 5] explore token merging, which can be viewed as another form of pruning. For our method, this approach did

		Method	Acc.	GFLOPs	TP (imgs/s)	
High Token Regime	GFLOPs ≥ 8.0	Deit-B-Distil. [19]	82.55	17.68	379	
		Top-K [15]	81.82	13.18	504	
		Zero-TP [21]	81.92	13.10	433	
		DynamicViT [17]	80.91	13.34	498	
		ToMe [5]	81.86	12.11	508	
		TNT (ours)	81.97	13.11	509	
	GFLOPs ≥ 2.0	Deit-S-Distil. [19]	80.49	4.63	1150	
		Top-K [15]	79.81	3.44	1496	
		Zero-TP [21]	79.66	3.42	983	
		DynamicViT [17]	79.45	3.47	1448	
		ToMe [5]	80.12	3.45	1281	
		TNT (ours)	79.89	3.41	1443	
	GFLOPs ≥ 4.0	ViT/16 [8]	78.70	9.17	644	
		Zero-TP [21]	77.07	6.75	688	
		ToMe [5]	77.03	6.97	734	
		TNT (ours)	77.32	6.73	842	
	Low Token Regime	GFLOPs < 8.0	Deit-B-Distil. [19]	82.55	17.68	379
			Top-K [15]	55.98	5.93	1084
Zero-TP [21]			19.76	6.18	731	
DynamicViT [17]			11.20	5.79	1102	
ToMe [5]			43.37	5.89	995	
TNT (ours)			59.93	5.87	1095	
GFLOPs < 2.0		Deit-S-Distil. [19]	80.49	4.63	1150	
		Top-K [15]	58.20	1.57	3003	
		Zero-TP [21]	27.75	1.63	1485	
		DynamicViT [17]	24.51	1.52	3037	
		ToMe [5]	62.88	1.55	2486	
		TNT (ours)	63.82	1.53	2973	
GFLOPs < 4.0		ViT/16 [8]	78.70	9.17	644	
		Zero-TP [21]	0.63	3.26	1179	
		ToMe [5]	6.30	3.26	1485	
		TNT (ours)	13.42	2.98	1786	

Table 2. Top-1 Accuracy on the ImageNet-1K validation set (**Acc.**) and computation cost measured by GFLOPs and throughput (**TP**), for DeiT-B-Distil., DeiT-S-Distil., and ViT/16, in two different computing regimes (“High” and “Low”, defined for each base model).

not give an improvement over similarity pruning.

4.4. Limitations

While the proposed TNT method provides relatively improved performance over other methods, important gaps remain in methodology. In this method, redundant tokens are not removed during training; while this can be performed through merging as in ToMe [5], as experimental results show it is difficult to do in a stable manner. Further, synergistic information between tokens is not considered; this seems less relevant to ImageNet classification, but likely would be useful in more complicated label structures (e.g., hierarchical/multi-class structures). This is also perhaps a

Method	Acc.	GFLOPs	TP (imgs/s)
DeiT-B-Distil. [19](SL)	82.55	17.68	379
TNT w/o Sim. Pruning	81.33	12.29	546
TNT (Seq. Part.)	81.52	12.30	536
TNT (Token Merge)	81.54	12.30	538
TNT (Random Part.)	81.57	12.30	542
DeiT-B-Distil. [19](ML)	82.55	17.68	379
TNT w/o Sim. Pruning	80.55	11.03	605
TNT (Token Merge)	81.41	11.41	575
TNT (Random Part.)	81.50	11.41	581

Table 3. Ablation study for TNT in DeiT-S-Distil. “SL” is single-layer pruning; “ML” is multi-layer pruning; **Acc.** is **Top-1 Accuracy**, **TP** is the **Throughput**, measured in images-per-second.

deeper problem than redundant tokens, as it has combinatorial complexity in the order of the interactions considered.

Beyond this, for better comparison measurements multi-layer dropping should be tuned for each method. This is prohibitively expensive, but could provide some less stable but higher capacity methods with a boost in performance.

Finally, in a deployment setting, hardware constraints will dictate keep-rates, which could be optimized for in the base-models directly (i.e., we could optimize a ViT for a 50% keep rate, or for a specific memory structure). This optimization was not done here, nor do we propose any candidate deployment device constraints, but nevertheless should be considered for best performance.

5. Conclusion

In this work, we introduced a novel token pruning method within the Information Bottleneck framework, aiming to optimize vision transformers by continuous optimization of token pruning. Our extensive evaluations on the ImageNet dataset using ViT and DeiT architectures demonstrate state-of-the-art performance in the accuracy-computation trade-off compared to existing methods. Specifically, our method excels in low-token retention rates, maintaining high accuracy while significantly reducing computational loads. These results underscore the potential impact of our method in improving the efficiency of deploying vision transformers, particularly in resource-constrained applications.

References

- [1] Alessandro Achille and Stefano Soatto. Information dropout: Learning optimal representations through noisy computation. *IEEE transactions on pattern analysis and machine intelligence*, 40(12):2897–2905, 2018. 3
- [2] Alexander A Alemi, Ian Fischer, Joshua V Dillon, and Kevin Murphy. Deep variational information bottleneck. *arXiv preprint arXiv:1612.00410*, 2016. 2, 3
- [3] Richard Blahut. Computation of channel capacity and rate-

- distortion functions. *IEEE transactions on Information Theory*, 18(4):460–473, 1972. 2
- [4] Daniel Bolya and Judy Hoffman. Token merging for fast stable diffusion. In *Proceedings of the IEEE/CVF conference on computer vision and pattern recognition*, pages 4599–4603, 2023. 7
 - [5] Daniel Bolya, Cheng-Yang Fu, Xiaoliang Dai, Peizhao Zhang, Christoph Feichtenhofer, and Judy Hoffman. Token merging: Your vit but faster. *arXiv preprint arXiv:2210.09461*, 2022. 2, 4, 5, 6, 7, 8, 1, 9, 10, 11, 12, 13, 14, 15, 16
 - [6] Thomas M Cover. *Elements of information theory*. John Wiley & Sons, 1999. 3
 - [7] Jia Deng, Wei Dong, Richard Socher, Li-Jia Li, Kai Li, and Li Fei-Fei. Imagenet: A large-scale hierarchical image database. In *2009 IEEE conference on computer vision and pattern recognition*, pages 248–255. Ieee, 2009. 4
 - [8] Alexey Dosovitskiy. An image is worth 16x16 words: Transformers for image recognition at scale. *arXiv preprint arXiv:2010.11929*, 2020. 1, 4, 8
 - [9] Mohsen Fayyaz, Soroush Abbasi Koohpayegani, Farnoush Rezaei Jafari, Sunando Sengupta, Hamid Reza Vaezi Joze, Eric Sommerlade, Hamed Pirsiavash, and Jürgen Gall. Adaptive token sampling for efficient vision transformers. In *European Conference on Computer Vision*, pages 396–414. Springer, 2022. 4
 - [10] Saurabh Goyal, Anamitra Roy Choudhury, Saurabh Raje, Venkatesan Chakaravarthy, Yogish Sabharwal, and Ashish Verma. Power-bert: Accelerating bert inference via progressive word-vector elimination. In *International Conference on Machine Learning*, pages 3690–3699. PMLR, 2020. 1
 - [11] Joakim Bruslund Haurum, Sergio Escalera, Graham W Taylor, and Thomas B Moeslund. Which tokens to use? investigating token reduction in vision transformers. In *Proceedings of the IEEE/CVF International Conference on Computer Vision*, pages 773–783, 2023. 2, 4, 5
 - [12] Gyuwan Kim and Kyunghyun Cho. Length-adaptive transformer: Train once with length drop, use anytime with search. *arXiv preprint arXiv:2010.07003*, 2020. 1
 - [13] Sehoon Kim, Sheng Shen, David Thorsley, Amir Gholami, Woosuk Kwon, Joseph Hassoun, and Kurt Keutzer. Learned token pruning for transformers. In *Proceedings of the 28th ACM SIGKDD Conference on Knowledge Discovery and Data Mining*, pages 784–794, 2022. 1
 - [14] Diederik P Kingma. Auto-encoding variational bayes. *arXiv preprint arXiv:1312.6114*, 2013. 3
 - [15] Youwei Liang, Chongjian Ge, Zhan Tong, Yibing Song, Jue Wang, and Pengtao Xie. Not all patches are what you need: Expediting vision transformers via token reorganizations. *arXiv preprint arXiv:2202.07800*, 2022. 1, 2, 8, 5, 9, 11, 12, 13
 - [16] Lawrence Page. The pagerank citation ranking: Bringing order to the web. Technical report, Technical Report, 1999. 2
 - [17] Yongming Rao, Wenliang Zhao, Benlin Liu, Jiwen Lu, Jie Zhou, and Cho-Jui Hsieh. Dynamicvit: Efficient vision transformers with dynamic token sparsification. *Advances in neural information processing systems*, 34:13937–13949, 2021. 1, 4, 6, 7, 8, 5, 9, 10, 11, 12, 13
 - [18] Naftali Tishby, Fernando C Pereira, and William Bialek. The information bottleneck method. *arXiv preprint physics/0004057*, 2000. 2, 3
 - [19] Hugo Touvron, Matthieu Cord, Matthijs Douze, Francisco Massa, Alexandre Sablayrolles, and Hervé Jégou. Training data-efficient image transformers & distillation through attention. In *International conference on machine learning*, pages 10347–10357. PMLR, 2021. 1, 4, 8
 - [20] A Vaswani. Attention is all you need. *Advances in Neural Information Processing Systems*, 2017. 1
 - [21] Hongjie Wang, Bhishma Dedhia, and Niraj K Jha. Zero-tp prune: Zero-shot token pruning through leveraging of the attention graph in pre-trained transformers. In *Proceedings of the IEEE/CVF Conference on Computer Vision and Pattern Recognition*, pages 16070–16079, 2024. 1, 2, 4, 5, 6, 7, 8, 9, 10, 11, 12, 13, 14, 15, 16
 - [22] Yifan Xu, Zhijie Zhang, Mengdan Zhang, Kekai Sheng, Ke Li, Weiming Dong, Liqing Zhang, Changsheng Xu, and Xing Sun. Evo-vit: Slow-fast token evolution for dynamic vision transformer. In *Proceedings of the AAAI Conference on Artificial Intelligence*, pages 2964–2972, 2022. 6
 - [23] Hongxu Yin, Arash Vahdat, Jose M Alvarez, Arun Mallya, Jan Kautz, and Pavlo Molchanov. A-vit: Adaptive tokens for efficient vision transformer. In *Proceedings of the IEEE/CVF conference on computer vision and pattern recognition*, pages 10809–10818, 2022. 1, 5

Training Noise Token Pruning

Supplementary Material

A. Implementation Code

Figure 6 is an implementation of our “VisionTransformer-WithTNT” in PyTorch.

B. Additional Experiment Details

Full results for plots and tables in the main paper including DeiT-Tiny-Distil. [19]. For all results, **Acc.** is Top-1 Accuracy, **TP** is the Throughput, measured in images-per-second.

Single-layer pruning settings: **K** is the keep rate. We divide K values into two tables: $K = 0.8$ to 0.45 represent the high-token regime, while $K = 0.4$ to 0.2 correspond to the low-token regime. Highlighted rows achieve the highest accuracy in a specific token regime. For Top-K [15], GFLOPs is relatively smaller as pruning occurs in the middle of the Transformer block. For clarity in visualizations of the computation-accuracy trade-off, data of Top-K corresponding to $K=0.2$ is omitted from the plots but is reported in the table.

Multi-layer pruning settings: For TNT, Top-K [15], and Zero-TP [21], **Loc** and **Rate** denote the pruning locations (layers) and the pruning rate at each layer, respectively. **itr** is an additional parameter for Zero-TP only, which specifies the number of iterations for the PageRank algorithm at each pruning layer. For ToMe [5], pruning is performed at every layer, with **r** representing the number of tokens pruned per layer. To ensure GFLOPs alignment for better comparison, we only collect 8 data points per base model for ToMe (10 for other models). For DynamicViT [17], the keep rates for the three pruning layers are specified as $[\rho, \rho^2, \rho^3]$. **Rate**, **r**, and **ρ** vary across different experiments.

Table 4 provides an overview of the fixed hyperparameters used consistently in all experiments. For different base models, we conduct the hyperexperiments using the same set of parameters.

Method	Param.
Top-K [15]	loc=[3, 4, 5]
Zero-TP [21]	itr(single-layer)=50 loc=[1, 3, 6, 9, 11] itr(multi-layer)=[30, 5, 5, 1, 1]
DynamicViT [17]	loc=[3, 6, 9]
ToMe [5]	loc[1:12]
TNT (ours)	loc=[3, 4, 5]

Table 4. overview of the fixed hyperparameters used consistently in all experiments.

B.1. Base Model: DeiT-Base-Distil.

For single-layer pruning, high-token regime results are listed in Table 5; low-token regime results are listed in Table 6. For multi-layer pruning, high-token regime results are listed in Table 7; low-token regime results are listed in Table 8.

	Method	Acc.	GFLOPs	TP (imgs/s)
	DeiT-B-Distil.	82.55	17.68	379
$K = 0.8$	Random Drop	81.59	14.93	-
	Top-K [15]	82.16	14.74	462
	Zero-TP [21]	82.25	14.95	411
	DynamicViT [17]	80.87	15.33	438
	ToMe [5]	81.86	14.74	447
	TNT (ours)	82.31	14.93	455
$K = 0.7$	Random Drop	80.79	13.64	-
	Top-K [15]	81.63	13.36	507
	Zero-TP [21]	81.74	13.67	448
	DynamicViT [17]	80.66	14.00	481
	ToMe [5]	80.80	13.36	493
	TNT (ours)	82.05	13.64	495
$K = 0.6$	Random Drop	79.59	12.29	-
	Top-K [15]	80.70	11.92	558
	Zero-TP [21]	80.58	12.32	488
	DynamicViT [17]	80.02	12.61	526
	ToMe [5]	78.28	11.92	546
	TNT (ours)	81.57	12.30	542
$K = 0.5$	Random Drop	77.72	11.02	-
	Top-K [15]	79.25	10.56	635
	Zero-TP [21]	78.63	11.05	540
	DynamicViT [17]	79.06	11.31	588
	ToMe [5]	71.57	10.56	621
	TNT (ours)	80.62	11.03	605
$K = 0.45$	Random Drop	76.23	10.35	-
	Top-K [15]	78.06	9.85	677
	Zero-TP [21]	77.15	10.38	571
	DynamicViT [17]	78.26	10.63	624
	TNT (ours)	79.85	10.31	640

Table 5. **Single-layer pruning** for DeiT-B-Distil. in high-token regime.

B.2. Base Model: DeiT-Small-Distil.

For single-layer pruning, high-token regime results are listed in Table 9; low-token regime results are listed in Table 10. For multi-layer pruning, high-token regime results are listed in Table 11; low-token regime results are listed in Table 12.


```

1 class VisionTransformerWithTNT(VisionTransformer):
2     def __init__(self, *args, **kwargs):
3         super().__init__(*args, **kwargs)
4         # Parameters introduced: Add alpha heads to produce noise signal term
5         self.alpha_norm = kwargs['norm_layer'](self.embed_dim)
6         self.alpha_heads = nn.ModuleList([
7             nn.Linear(self.embed_dim, 1) for _ in range(kwargs['depth'])
8         ])
9         self.alpha_heads.apply(self._init_weights)
10
11     def forward_features(self, x):
12         B = x.shape[0]
13         x = self.patch_embed(x)
14
15         cls_tokens = self.cls_token.expand(B, -1, -1)
16         x = torch.cat((cls_tokens, x), dim=1)
17         x = x + self.pos_embed
18         x = self.pos_drop(x)
19         for i, (blk, alpha_head) in enumerate(zip(self.blocks, self.alpha_heads)):
20             x = blk(x)
21             # Noise allocator: To add noise to token embeddings at 1-5 layers while fine-tuning
22             if self.training and i < 5:
23                 alpha = alpha_head(x[:, 1:])
24                 alpha = torch.softmax(alpha.squeeze(-1), dim=-1)
25                 alpha = 1 - alpha
26                 noise = torch.randn_like(x[:, 1:]) * alpha.unsqueeze(-1).repeat(1, 1, x.size(-1))
27                 zero_noise = torch.zeros_like(cls_tokens)
28                 noise = torch.cat((zero_noise, noise), dim=1)
29                 x = self.alpha_norm(x)
30                 x = x + 0.02 * noise
31         x = self.norm(x)
32         return x[:, 0]
33
34     def forward(self, x):
35         x = self.forward_features(x)
36         x = self.head(x)
37         return x

```

Figure 6. Python implementation of **VisionTransformerWithTNT** class. Codes highlighted with brown are the main modifications. **VisionTransformer** class is taken from https://github.com/rwightman/pytorch-image-models/blob/master/timm/models/vision_transformer.py. We make simple modifications to allocate noise to token embeddings while fine-tuning.

B.3. Base Model: DeiT-Tiny-Distil.

Figure 7 shows the plots for DeiT-Tiny-Distil.. For single-layer pruning, high-token regime results are listed in Table 13; low-token regime results are listed in Table 14. For multi-layer pruning, high-token regime results are listed in Table 15; low-token regime results are listed in Table 16.

B.4. Base Model: ViT/16

For ViT/16, we use the mean-pooled tokens for the prediction rather than using CLS token. Therefore, Top-K is not applicable. We instead sweep the number of tokens (denoted as **#tokens**) from 160 to 50. #Tokens from 160 to 110 represent the high-token regime while #tokens from 100 to 50 correspond to low-token regime. For single-layer pruning, high-token regime results are listed in Table 17; low-token regime results are listed in Table 18. For multi-layer pruning, high-token regime results are listed in Table 19; low-token

regime results are listed in Table 20.

C. More examples for visualization

More qualitative results for pruning 50% of tokens at varying layers (single-layer pruning at layers 1-5) on the ImageNet-1K validation dataset in Figure 8.

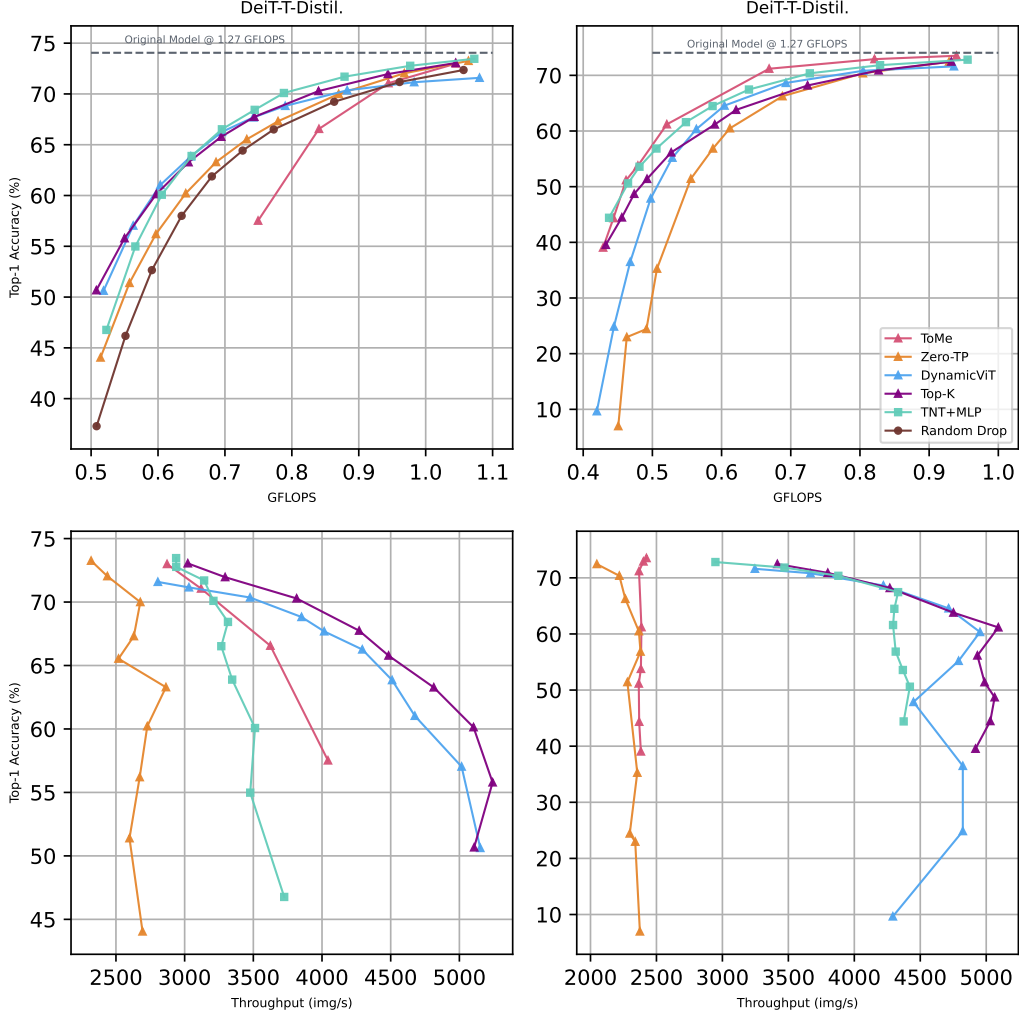


Figure 7. **Experimental Results for DeiT-Tiny-Distil.** We plot the Top-1 Accuracy in the ImageNet-1k validation set for each of the pruning methods as a function of computational efficiency, in the **top row** measured by GFLOPs and in the **bottom row** measured by throughput, for **multi-layer pruning**. For weaker encoders and/or smaller transformer blocks such as DeiT-Tiny, we rather use MLP, which means less parallelism. The throughput of models in multi-layer pruning reaches approximately 5000 images per second, potentially limited by hardware bottlenecks.



Figure 8. More Visualization of Token Pruning maps on ImageNet-1K: at **left** are the original images, and at each column **progressing right** are single layer prunings and their associated kept/dropped tokens, for layers 1-5 of the DeiT-S-Distil. model.

	Method	Acc.	GFLOPs	TP (imgs/s)
	DeiT-B-Distil.	82.55	17.68	379
$K = 0.4$	Random Drop	74.08	9.70	-
	Top-K [15]	76.53	9.14	728
	Zero-TP [21]	75.15	9.72	603
	Dynamic ViT [17]	77.01	9.95	668
	TNT (ours)	78.89	9.70	684
$K = 0.35$	Random Drop	70.57	9.04	-
	Top-K [15]	74.26	8.43	786
	Zero-TP [21]	72.32	9.06	649
	Dynamic ViT [17]	75.28	9.27	710
	TNT (ours)	77.22	9.04	723
$K = 0.3$	Random Drop	64.89	8.38	-
	Top-K [15]	70.68	7.73	853
	Zero-TP [21]	68.68	8.41	680
	Dynamic ViT [17]	72.69	8.59	770
	TNT (ours)	74.75	8.38	786
$K = 0.25$	Random Drop	57.12	7.80	-
	Top-K [15]	65.95	7.10	925
	Zero-TP [21]	63.62	7.82	717
	Dynamic ViT [17]	68.87	7.99	823
	TNT (ours)	70.76	7.80	834
$K = 0.2$	Random Drop	44.17	7.14	-
	Top-K [15]	57.51	6.40	1016
	Zero-TP [21]	55.28	7.17	779
	Dynamic ViT [17]	61.86	7.32	904
	TNT (ours)	62.62	7.15	907

Table 6. **Single-layer pruning** for DeiT-B-Distil. in low-token regime.

	Method	Acc.	GFLOPs	TP (imgs/s)	Param.
	DeiT-B-Distil.	82.55	17.68	379	-
GFLOPs \approx 13.0	Top-K	81.82	13.18	503	Rate=[.9, .9, .8]
	Zero-TP [21]	81.92	13.10	433	Rate=[1., .9, .9, .9, 1.]
	DynamicViT [17]	80.91	13.34	498	$\rho=.8$
	ToMe [5]	81.86	12.11	508	$r=8$
	TNT (ours)	81.97	13.11	509	Rate=[1., .95, .95]
GFLOPs \approx 11.5	Top-K	80.96	11.72	581	Rate=[.85, .8, .8]
	Zero-TP [21]	80.97	11.37	424	Rate=[1., .8, .8, .9, 1.]
	DynamicViT [17]	80.67	11.49	576	$\rho=.7$
	ToMe [5]	81.71	11.56	533	$r=11$
	TNT (ours)	81.50	11.41	581	Rate=[.9, .9, .9]
GFLOPs \approx 10.0	Top-K	79.63	10.25	650	Rate=[.85, .7, .7]
	Zero-TP [21]	78.77	9.71	573	Rate=[1., .7, .7, .8, 1.]
	DynamicViT [17]	79.55	9.88	659	$\rho=.6$
	ToMe [5]	80.51	9.39	651	$r=15$
	TNT (ours)	80.56	10.01	660	Rate=[.85, .85, .8]
GFLOPs \approx 8.5	Top-K	76.84	8.75	748	Rate=[.7, .7, .65]
	Zero-TP [21]	75.60	8.61	613	Rate=[1., .6, .7, .7, 1.]
	DynamicViT [17]	76.73	8.57	761	$\rho=.5$
	TNT (ours)	78.96	8.77	758	Rate=[.75, .85, .7]
GFLOPs \approx 8.0	Top-K	75.04	8.14	814	Rate=[.65, .65, .65]
	Zero-TP [21]	73.32	8.22	636	Rate=[1., .6, .6, .7, 1.]
	DynamicViT [17]	73.71	7.96	817	$\rho=.45$
	TNT (ours)	77.31	8.03	822	Rate=[.65, .85, .7]

Table 7. **Multi-layer pruning** for DeiT-B-Distil. in high-token regime.

	Method	Acc.	GFLOPs	TP (imgs/s)	Param.
	DeiT-B-Distil.	82.55	17.68	379	-
GFLOPs \approx 7.5	Top-K	71.59	7.37	881	Rate=[.6, .6, .6]
	Zero-TP [21]	69.66	7.76	654	Rate=[1., .5, .5, .6, 1.]
	DynamicViT [17]	68.79	7.45	877	$\rho=.4$
	ToMe [5]	72.29	7.23	823	$r=20$
	TNT (ours)	75.33	7.49	871	Rate=[.6, .8, .7]
GFLOPs \approx 7.0	Top-K	67.51	6.84	948	Rate=[.6, .5, .6]
	Zero-TP [21]	55.65	7.03	703	Rate=[1., .4, .4, .4, 1.]
	DynamicViT [17]	60.30	6.97	926	$\rho=.35$
	ToMe [5]	68.53	6.91	855	$r=21$
	TNT (ours)	71.92	6.89	947	Rate=[.5, .8, .7]
GFLOPs \approx 6.6	Top-K	65.24	6.56	993	Rate=[.55, .5, .6]
	Zero-TP [21]	43.24	6.79	735	Rate=[1., .4, .3, .4, 1.]
	DynamicViT [17]	45.65	6.53	982	$\rho=.3$
	ToMe [5]	64.33	6.62	893	$r=22$
	TNT (ours)	69.06	6.53	991	Rate=[.5, .7, .7]
GFLOPs \approx 6.2	Top-K	61.54	6.29	1044	Rate=[.55, .5, .5]
	Zero-TP [21]	39.17	6.37	762	Rate=[1., .3, .4, .4, 1.]
	DynamicViT [17]	29.87	6.17	1043	$\rho=.25$
	ToMe [5]	51.32	6.11	962	$r=24$
	TNT (ours)	66.21	6.28	1039	Rate=[.5, .7, .6]
GFLOPs \approx 5.7	Top-K	55.98	5.93	1084	Rate=[.5, .45, .5]
	Zero-TP [21]	19.76	6.18	731	Rate=[1., .3, .3, .4, 1.]
	DynamicViT [17]	11.20	5.79	1102	$\rho=.2$
	ToMe [5]	43.37	5.89	995	$r=25$
	TNT (ours)	59.93	5.87	1095	Rate=[.5, .6, .55]

Table 8. **Multi-layer pruning** for DeiT-B-Distil. in low-token regime.

	Method	Acc.	GFLOPs	TP (imgs/s)
	DeiT-S-Distil.	80.49	4.63	1150
K = 0.8	Random Drop	79.54	3.90	-
	Top-K [15]	80.12	3.85	1338
	Zero-TP [21]	79.99	3.91	1156
	DynamicViT [17]	79.39	3.99	1255
	ToMe [5]	80.07	3.85	1290
	TNT (ours)	80.11	3.90	1316
K = 0.7	Random Drop	78.91	3.55	-
	Top-K [15]	79.69	3.48	1478
	Zero-TP [21]	79.55	3.57	1243
	DynamicViT [17]	79.25	3.64	1381
	ToMe [5]	79.24	3.49	1415
	TNT (ours)	79.82	3.56	1427
K = 0.6	Random Drop	77.83	3.20	-
	Top-K [15]	78.89	3.11	1655
	Zero-TP [21]	78.94	3.21	1343
	DynamicViT [17]	78.66	3.28	1528
	ToMe [5]	77.40	3.11	1596
	TNT (ours)	79.29	3.20	1587
K = 0.5	Random Drop	76.57	2.87	-
	Top-K [15]	77.69	2.75	1854
	Zero-TP [21]	77.74	2.88	1463
	DynamicViT [17]	77.96	2.94	1706
	ToMe [5]	73.13	2.75	1791
	TNT (ours)	78.65	2.87	1768
K = 0.45	Random Drop	75.61	2.69	-
	Top-K [15]	76.70	2.57	1995
	Zero-TP [21]	76.97	2.71	1514
	DynamicViT [17]	77.22	2.76	1800
	TNT (ours)	78.06	2.70	1878

Table 9. **Single-layer pruning** for DeiT-S-Distil. in high-token regime.

	Method	Acc.	GFLOPs	TP (imgs/s)
	DeiT-S-Distil.	80.49	4.63	1150
K = 0.4	Random Drop	74.57	2.52	-
	Top-K [15]	75.45	2.38	2143
	Zero-TP [21]	75.91	2.54	1605
	DynamicViT [17]	76.40	2.58	1934
	TNT (ours)	77.32	2.52	1994
K = 0.35	Random Drop	72.79	2.35	-
	Top-K [15]	73.87	2.20	2342
	Zero-TP [21]	74.58	2.37	1679
	DynamicViT [17]	75.22	2.41	2091
	TNT (ours)	76.19	2.35	2167
K = 0.3	Random Drop	70.42	2.18	-
	Top-K [15]	71.60	2.02	2465
	Zero-TP [21]	72.70	2.20	1711
	DynamicViT [17]	73.41	2.24	2189
	TNT (ours)	74.65	2.19	2269
K = 0.25	Random Drop	67.77	2.03	-
	Top-K [15]	68.57	1.86	2713
	Zero-TP [21]	69.99	2.05	1757
	DynamicViT [17]	71.03	2.08	2376
	TNT (ours)	72.66	2.03	2444
K = 0.2	Random Drop	62.83	1.87	-
	Top-K [15]	64.12	1.68	2842
	Zero-TP [21]	65.90	1.88	1797
	DynamicViT [17]	66.67	1.91	2496
	TNT (ours)	69.08	1.87	2552

Table 10. **Single-layer pruning** for DeiT-S-Distil. in low-token regime.

	Method	Acc.	GFLOPs	TP (imgs/s)	Param.
	DeiT-S-Distil.	80.49	4.63	1150	-
GFLOPs \approx 3.45	Top-K [15]	79.81	3.44	1496	Rate=[.9, .9, .8]
	Zero-TP [21]	79.66	3.42	983	Rate=[1., .9, .9, .9, 1.]
	DynamicViT [17]	79.45	3.47	1448	$\rho=.8$
	ToMe [5]	80.12	3.45	1281	$r=8$
	TNT (ours)	79.89	3.41	1444	Rate=[1., .95, .95]
GFLOPs \approx 3.0	Top-K [15]	79.11	3.06	1706	Rate=[.85, .8, .8]
	Zero-TP [21]	78.75	2.97	1171	Rate=[1., .8, .8, .9, 1.]
	DynamicViT [17]	79.18	2.99	1679	$\rho=.7$
	ToMe [5]	79.86	3.02	1448	$r=11$
	TNT (ours)	79.38	2.97	1652	Rate=[.9, .9, .9]
GFLOPs \approx 2.6	Top-K [15]	77.65	2.67	1909	Rate=[.85, .7, .7]
	Zero-TP [21]	76.92	2.54	1352	Rate=[1., .7, .7, .8, 1.]
	DynamicViT [17]	78.38	2.57	1929	$\rho=.6$
	ToMe [5]	79.12	2.54	1754	$r=15$
	TNT (ours)	78.57	2.60	1882	Rate=[.85, .85, .8]
GFLOPs \approx 2.25	Top-K [15]	75.33	2.29	2190	Rate=[.7, .7, .65]
	Zero-TP [21]	74.35	2.25	1389	Rate=[1., .6, .7, .7, 1.]
	DynamicViT [17]	76.39	2.23	2192	$\rho=.5$
	TNT (ours)	77.25	2.28	2143	Rate=[.75, .85, .7]
GFLOPs \approx 2.1	Top-K [15]	73.73	2.13	2343	Rate=[.65, .65, .65]
	Zero-TP [21]	72.55	2.16	1415	Rate=[1., .6, .6, .7, 1.]
	DynamicViT [17]	74.41	2.08	2321	$\rho=.45$
	TNT (ours)	75.93	2.09	2302	Rate=[.65, .85, .7]

Table 11. **Multi-layer pruning** for DeiT-S-Distil. in high-token regime.

	Method	Acc.	GFLOPs	TP (imgs/s)	Param.
	DeiT-S-Distil.	80.49	4.63	1150	-
GFLOPs ≈ 1.95	Top-K	70.78	1.93	2525	Rate=[.6, .6, .6]
	Zero-TP [21]	69.48	2.03	1357	Rate=[1., .5, .5, .6, 1.]
	DynamicViT [17]	71.69	1.95	2490	$\rho=.4$
	ToMe [5]	74.76	1.90	2176	$r=20$
	TNT (ours)	74.54	1.95	2484	Rate=[.6, .8, .7]
GFLOPs ≈ 1.8	Top-K	67.34	1.80	2701	Rate=[.6, .5, .6]
	Zero-TP [21]	59.29	1.85	1331	Rate=[1., .4, .4, .4, 1.]
	DynamicViT [17]	67.03	1.83	2635	$\rho=.35$
	ToMe [5]	71.50	1.74	2351	$r=21$
	TNT (ours)	72.26	1.79	2639	Rate=[.5, .8, .7]
GFLOPs ≈ 1.75	Top-K	65.55	1.73	2794	Rate=[.55, .5, .6]
	Zero-TP [21]	49.70	1.79	1471	Rate=[1., .4, .3, .4, 1.]
	DynamicViT [17]	58.70	1.71	2761	$\rho=.3$
	ToMe [5]	69.76	1.68	2377	$r=22$
	TNT (ours)	70.31	1.70	2725	Rate=[.5, .7, .7]
GFLOPs ≈ 1.65	Top-K	62.41	1.66	2896	Rate=[.55, .5, .5]
	Zero-TP [21]	48.44	1.68	1481	Rate=[1., .3, .4, .4, 1.]
	DynamicViT [17]	47.71	1.62	2943	$\rho=.25$
	ToMe [5]	66.30	1.61	2357	$r=24$
	TNT (ours)	68.36	1.64	2850	Rate=[.5, .7, .6]
GFLOPs ≈ 1.55	Top-K	58.20	1.57	3003	Rate=[.5, .45, .5]
	Zero-TP [21]	27.75	1.63	1485	Rate=[1., .3, .3, .4, 1.]
	DynamicViT [17]	24.51	1.52	3037	$\rho=.2$
	ToMe [5]	62.88	1.55	2486	$r=25$
	TNT (ours)	63.82	1.53	2973	Rate=[.5, .6, .55]

Table 12. **Multi-layer pruning** for DeiT-S-Distil. in low-token regime.

	Method	Acc.	GFLOPs	TP (imgs/s)
	DeiT-T-Distil.	74.05	1.27	2607
K = 0.8	Random Drop	72.36	1.06	-
	Top-K [15]	73.05	1.04	3023
	Zero-TP [21]	73.25	1.06	2319
	DynamicViT [17]	71.59	1.08	2805
	ToMe [5]	72.99	1.05	2872
	TNT+MLP (ours)	73.46	1.07	2938
K = 0.7	Random Drop	71.17	0.96	-
	Top-K [15]	71.96	0.94	3295
	Zero-TP [21]	72.03	0.97	2438
	DynamicViT [17]	71.15	0.98	3031
	ToMe [5]	71.06	0.94	3120
	TNT+MLP (ours)	72.77	0.98	2939
K = 0.6	Random Drop	69.23	0.86	-
	Top-K [15]	70.28	0.84	3815
	Zero-TP [21]	69.99	0.87	2677
	DynamicViT [17]	70.36	0.88	3476
	ToMe [5]	66.56	0.84	3624
	TNT+MLP (ours)	71.70	0.88	3142
K = 0.5	Random Drop	66.50	0.77	-
	Top-K [15]	67.74	0.74	4270
	Zero-TP [21]	67.31	0.78	2630
	DynamicViT [17]	68.82	0.79	3851
	ToMe [5]	57.52	0.75	4043
	TNT+MLP (ours)	70.09	0.79	3210
K = 0.45	Random Drop	64.43	0.73	-
	Top-K [15]	65.78	0.69	4484
	Zero-TP [21]	65.54	0.73	2519
	DynamicViT [17]	67.69	0.74	4016
	TNT+MLP (ours)	68.43	0.74	3315

Table 13. **Single-layer pruning** for DeiT-T-Distil. in low-token regime.

	Method	Acc.	GFLOPs	TP (imgs/s)
	DeiT-T-Distil.	74.05	1.27	2607
K = 0.4	Random Drop	61.88	0.68	-
	Top-K [15]	63.27	0.65	4814
	Zero-TP [21]	63.29	0.69	2864
	DynamicViT [17]	66.26	0.70	4293
	TNT+MLP (ours)	66.52	0.70	3267
K = 0.35	Random Drop	57.99	0.64	-
	Top-K [15]	60.13	0.60	5103
	Zero-TP [21]	60.21	0.64	2728
	DynamicViT [17]	63.85	0.65	4510
	TNT+MLP (ours)	63.89	0.65	3346
K = 0.3	Random Drop	52.65	0.59	-
	Top-K [15]	55.79	0.55	5242
	Zero-TP [21]	56.20	0.60	2673
	DynamicViT [17]	61.03	0.60	4676
	TNT+MLP (ours)	60.08	0.61	3512
K = 0.25	Random Drop	46.18	0.55	-
	Top-K [15]	50.67	0.51	5108
	Zero-TP [21]	51.39	0.56	2598
	DynamicViT [17]	57.03	0.56	5016
	TNT+MLP (ours)	54.98	0.57	3477
K = 0.2	Random Drop	37.29	0.51	-
	Top-K [15]	43.40	0.46	5153
	Zero-TP [21]	44.04	0.51	2694
	DynamicViT [17]	50.62	0.52	5152
	TNT+MLP (ours)	46.77	0.52	3725

Table 14. **Single-layer pruning** for DeiT-T-Distil. in low-token regime.

	Method	Acc.	GFLOPs	TP (imgs/s)	Param.
	DeiT-T-Distil.	74.05	1.27	2607	-
GFLOPs ≈ 0.93	Top-K [15]	72.46	0.93	3416	Rate=[.9, .9, .8]
	Zero-TP [21]	72.45	0.93	2048	Rate=[1., .9, .9, .9, 1.]
	DynamicViT [17]	71.61	0.94	3246	$\rho=.8$
	ToMe [5]	73.52	0.94	2424	$r=8$
	TNT+MLP (ours)	72.82	0.96	2947	Rate=[1., .95, .95]
GFLOPs ≈ 0.82	Top-K [15]	70.88	0.83	3799	Rate=[.85, .8, .8]
	Zero-TP [21]	70.36	0.80	2219	Rate=[1., .8, .8, .9, 1.]
	DynamicViT [17]	70.82	0.80	3668	$\rho=.7$
	ToMe [5]	72.91	0.82	2401	$r=11$
	TNT+MLP (ours)	71.83	0.83	3470	Rate=[.9, .9, .9]
GFLOPs ≈ 0.7	Top-K [15]	68.18	0.72	4269	Rate=[.85, .7, .7]
	Zero-TP [21]	66.24	0.69	2264	Rate=[1., .7, .7, .8, 1.]
	DynamicViT [17]	68.63	0.69	4220	$\rho=.6$
	ToMe [5]	71.19	0.67	2368	$r=15$
	TNT+MLP (ours)	70.36	0.73	3879	Rate=[.85, .85, .8]
GFLOPs ≈ 0.62	Top-K [15]	63.80	0.62	4751	Rate=[.7, .7, .65]
	Zero-TP [21]	60.48	0.61	2367	Rate=[1., .6, .7, .7, 1.]
	DynamicViT [17]	64.55	0.60	4715	$\rho=.5$
	TNT+MLP (ours)	67.45	0.64	4332	Rate=[.75, .85, .7]
GFLOPs ≈ 0.58	Top-K [15]	61.17	0.59	5092	Rate=[.65, .65, .65]
	Zero-TP [21]	56.84	0.59	2380	Rate=[1., .6, .6, .7, 1.]
	DynamicViT [17]	60.34	0.56	4953	$\rho=.45$
	TNT+MLP (ours)	64.48	0.59	4304	Rate=[.65, .85, .7]

Table 15. **Multi-layer pruning** for DeiT-T-Distil. in high-token regime.

	Method	Acc.	GFLOPs	TP (imgs/s)	Param.
	DeiT-T-Distil.	74.05	1.27	2607	-
GFLOPs ≈ 0.53	Top-K [15]	56.15	0.53	4933	Rate=[.6, .6, .6]
	Zero-TP [21]	51.41	0.56	2280	Rate=[1., .5, .5, .6, 1.]
	DynamicViT [17]	55.20	0.53	4790	$\rho=.4$
	ToMe [5]	61.20	0.52	2386	$r=20$
	TNT+MLP (ours)	61.59	0.55	4294	Rate=[.6, .8, .7]
GFLOPs ≈ 0.5	Top-K [15]	51.39	0.49	4987	Rate=[.6, .5, .6]
	Zero-TP [21]	35.26	0.51	2355	Rate=[1., .4, .4, .4, 1.]
	DynamicViT [17]	47.87	0.50	4448	$\rho=.35$
	ToMe [5]	53.77	0.48	2382	$r=21$
	TNT+MLP (ours)	56.85	0.51	4314	Rate=[.5, .8, .7]
GFLOPs ≈ 0.47	Top-K [15]	48.70	0.47	5064	Rate=[.55, .5, .6]
	Zero-TP [21]	24.42	0.49	2298	Rate=[1., .4, .3, .4, 1.]
	DynamicViT [17]	36.48	0.47	4823	$\rho=.3$
	ToMe [5]	51.15	0.46	2366	$r=22$
	TNT+MLP (ours)	53.58	0.48	4368	Rate=[.5, .7, .7]
GFLOPs ≈ 0.45	Top-K [15]	44.47	0.46	5031	Rate=[.55, .5, .5]
	Zero-TP [21]	22.97	0.46	2339	Rate=[1., .3, .4, .4, 1.]
	DynamicViT [17]	24.86	0.44	4823	$\rho=.25$
	ToMe [5]	44.34	0.44	2369	$r=24$
	TNT+MLP (ours)	50.60	0.46	4421	Rate=[.5, .7, .6]
GFLOPs ≈ 0.43	Top-K [15]	39.54	0.43	4919	Rate=[.5, .45, .5]
	Zero-TP [21]	6.97	0.45	2374	Rate=[1., .3, .3, .4, 1.]
	DynamicViT [17]	9.65	0.42	4292	$\rho=.2$
	ToMe [5]	39.05	0.43	2382	$r=25$
	TNT+MLP (ours)	44.41	0.44	4374	Rate=[.5, .6, .55]

Table 16. **Multi-layer pruning** for DeiT-T-Distil. in low-token regime.

#Tokens	Method	Acc.	GFLOPs	TP (imgs/s)
	ViT/16	78.70	9.17	644
160	Random Drop	77.17	7.69	-
	Zero-TP [21]	77.43	7.32	665
	ToMe [5]	77.71	7.66	752
	TNT (ours)	77.94	7.70	747
150	Random Drop	76.75	7.29	-
	Zero-TP [21]	76.80	6.92	687
	ToMe [5]	77.22	7.24	784
	TNT (ours)	77.64	7.30	779
140	Random Drop	76.00	6.89	-
	Zero-TP [21]	76.80	6.92	722
	ToMe [5]	76.53	6.83	838
	TNT (ours)	76.97	6.90	820
130	Random Drop	75.12	6.50	-
	Zero-TP [21]	75.96	6.52	749
	ToMe [5]	75.70	6.42	877
	TNT (ours)	76.22	6.50	856
120	Random Drop	73.79	6.10	-
	Zero-TP [21]	74.81	6.13	812
	ToMe [5]	74.19	6.02	969
	TNT (ours)	75.24	6.11	945
110	Random Drop	71.95	5.71	-
	Zero-TP [21]	73.26	5.74	863
	ToMe [5]	71.54	5.62	1047
	TNT (ours)	73.73	5.72	1016

Table 17. **Single-layer pruning** for ViT/16. in high-token regime.

#Tokens	Method	Acc.	GFLOPs	TP (imgs/s)
	ViT/16	78.70	9.17	644
100	Random Drop	69.21	5.33	-
	Zero-TP [21]	70.92	5.35	901
	ToMe [5]	66.46	5.22	1103
	TNT (ours)	71.69	5.33	1069
90	Random Drop	64.71	4.94	-
	Zero-TP [21]	67.40	4.97	960
	TNT (ours)	68.73	4.95	1153
80	Random Drop	57.64	4.56	-
	Zero-TP [21]	61.76	4.59	1002
	TNT (ours)	63.87	4.56	1247
70	Random Drop	46.28	4.18	-
	Zero-TP [21]	53.15	4.21	1021
	TNT (ours)	55.19	4.19	1344
60	Random Drop	31.16	3.81	-
	Zero-TP [21]	40.84	3.83	1157
	TNT (ours)	41.75	3.81	1457
50	Random Drop	16.57	3.44	-
	Zero-TP [21]	27.64	3.46	1228
	TNT (ours)	27.40	3.44	1531

Table 18. **Single-layer pruning** for ViT/16. in low-token regime.

	Method	Acc.	GFLOPs	TP (imgs/s)	Param.
	ViT/16	78.70	9.17	644	-
GFLOPs ≈ 6.8	Zero-TP [21]	77.07	6.75	688	Rate=[1., .9, .9, .9, 1.]
	ToMe [5]	77.02	6.97	734	$r=8$
	TNT (ours)	77.32	6.73	842	Rate=[1., .95, .95]
GFLOPs ≈ 6.00	Zero-TP [21]	75.16	5.84	778	Rate=[1., .8, .8, .9, 1.]
	ToMe [5]	77.02	6.14	823	$r=11$
	TNT (ours)	75.47	5.84	967	Rate=[.9, .9, .9]
GFLOPs ≈ 5.00	Zero-TP [21]	69.91	4.98	885	Rate=[1., .7, .7, .8, 1.]
	ToMe [5]	70.95	5.06	989	$r=15$
	TNT (ours)	72.23	5.10	1103	Rate=[.85, .85, .8]
GFLOPs ≈ 4.43	Zero-TP [21]	60.39	4.41	966	Rate=[1., .6, .7, .7, 1.]
	TNT (ours)	65.81	4.46	1249	Rate=[.75, .85, .7]
GFLOPs ≈ 4.10	Zero-TP [21]	51.96	4.25	994	Rate=[1., .6, .6, .7, 1.]
	TNT (ours)	58.96	4.08	1351	Rate=[.65, .85, .7]

Table 19. **Multi-layer pruning** for ViT/16. in high-token regime.

	Method	Acc.	GFLOPs	TP (imgs/s)	Param.
	ViT/16	78.70	9.17	644	-
GFLOPs \approx 3.90	Zero-TP [21]	40.38	3.98	1035	Rate=[1., .6, .6, .7, 1.]
	ToMe [5]	41.78	3.96	1243	$r=20$
	TNT (ours)	51.40	3.80	1452	Rate=[.65, .85, .7]
GFLOPs \approx 3.60	Zero-TP [21]	13.86	3.60	1092	Rate=[1., .5, .5, .6, 1.]
	ToMe [5]	22.58	3.64	1340	$r=21$
	TNT (ours)	39.81	3.50	1546	Rate=[.5, .8, .7]
GFLOPs \approx 3.40	Zero-TP [21]	5.15	3.48	1102	Rate=[1., .4, .3, .4, 1.]
	ToMe [5]	17.74	3.51	1382	$r=21$
	TNT (ours)	30.86	3.31	1626	Rate=[.5, .7, .7]
GFLOPs \approx 3.20	Zero-TP [21]	4.12	3.27	1163	Rate=[1., .3, .4, .4, 1.]
	ToMe [5]	9.19	3.37	1446	$r=24$
	TNT (ours)	23.71	3.18	1700	Rate=[.5, .7, .6]
GFLOPs \approx 3.10	Zero-TP [21]	0.64	3.17	1179	Rate=[1., .3, .3, .4, 1.]
	ToMe [5]	6.30	3.26	1485	$r=25$
	TNT (ours)	13.42	2.98	1786	Rate=[.5, .6, .55]

Table 20. **Multi-layer pruning** for ViT/16. in low-token regime.